Planetary Stationary Waves in the Atmosphere Part II: Thermal Stationary Waves

Yong. L. McHall
Department of Meteorology, University of Edinburgh, EH9 3JZ, U. K.
Received September 1, 1990; revised November 14, 1990

ABSTRACT

The contribution of thermal forcing to the planetary stationary waves will be studied also by assuming that heat balance in stationary waves over zonally asymmetric thermal forcing must be maintained over a long time period. Using the same model of geostrophic waves introduced in Part I, we may explain successfully the observed and simulated responses to the thermal forcing in the atmosphere, such as the wave 1 structure at high levels of middle latitudes, the seasonal changes of the stationary waves in the Northern Hemisphere, the opposite phase distributions of stationary waves at high and low levels of the subtropical regions in both hemispheres and so on.

I. INTRODUCTION

The effect of thermal forcing on stationary waves in the atmosphere has become major subject of many theoretical investigations and numerical experiments since the pioneering work of Smagorinsky (1953). In this work, however, the contribution of thermal forcing was not separated from that of orographic forcing. Though some aspects of the thermal contribution have been simulated separately with numerical models in later studies, it still remains a great difficulty to give a comprehensive physical interpretation for the thermal contribution in generation and maintenance of the stationary waves.

Since deviations of sea surface temperature from zonal symmetry on oceans and continents are reverted in phase from winter through summer, seasonal changes of thermal forcing may have important influences on stationary waves, at least in the Northern Hemisphere. The study on the contribution of thermal forcing must be able to explain the observed seasonal variations in stationary waves. However, most experiments devoted to the study before were designed particularly for the winter Northern Hemisphere. Thus, understanding of thermal stationary waves requires further investigation involving the seasonal changes in thermal forcing. The studies published before were generally far from this request.

We have studied in Part I the stationary waves excited by zonally asymmetric orographic forcing according to zonal momentum balance in these waves. The philosophy and techniques we used may be applied also for the study of thermal stationary waves. We hypothesize here that existence of thermal stationary waves is generated necessarily for heat balance with zonally asymmetric thermal forcing below over a long time period. The wave patterns are determined by the geostrophic perturbation equations as well. While, the long-term heat balance in thermal stationary waves will be studied analogously by using the primitive equation of thermodynamic energy. The obtained results may allow us to explain the distributions, structures and the seasonal changes of thermal stationary waves at different latitudes.

II. HEAT TRANSPORT

It will be revealed that the distribution of thermal stationary waves depends on the direction of heat flux. In this section, we discuss heat transport in geostrophic wave circulations.

The zonal mean flux of heat in the atmosphere through a surface of unit area parallel to the xp–plane within isobaric surfaces p and $p+g$ and with unit length along x direction is represented by

$$\overline{F_T} = C_p \overline{T_v} \ ,$$

where, v indicates three–dimensional velocity, and overbar signifies the zonal mean defined in Part I. In geostrophic wave circulations, we apply

$$T = \overline{T} - \frac{\delta\sigma_z}{R\sigma_y} mp\Phi e^{i(vt-kx+my+lp)}$$

and the other perturbations derived in Part I, producing

$$\frac{\overline{F_T}}{C_p} = \left(\overline{Tu} - \frac{\delta m^2 \sigma_z p}{2fR\sigma_y}\Phi^2\right)\hat{X} - \left(\frac{\delta km\sigma_z p}{2fR\sigma_y}\Phi^2 - \overline{Tv}\right)\hat{y} - \frac{\delta km}{2fR} p\Phi^2 \hat{\mathbf{P}} \ , \tag{1}$$

in which, $\hat{X}$, $\hat{y}$ and $\hat{\mathbf{P}}$ are unit vectors along corresponding coordinates. It is found by scale analyses that zonal transport of heat is along the same direction as mean zonal flow, while meridional flux is mainly contributed by eddies. The meridional and vertical eddy components are represented, respectively, by

$$\overline{F_{T_y}} = -\delta\frac{C_p km\sigma_z}{2fR\sigma_y} p\Phi^2 \ ,$$

$$\overline{F_{T_p}} = -\delta\frac{C_p km}{2fR} p\Phi^2 \ .$$

They show clearly that in the Northern Hemisphere, waves with northeast–southwest tilt of troughs transport heat upward and meridionally along the downgradient direction of mean temperature. While in the Southern Hemisphere, this downgradient transport takes place in the waves with troughs in the northwest–southeast direction. The magnitude of heat transport depends on wave parameters and mean atmospheric structures. Heat transport is more effective in the waves of short wavelength, great horizontal tilt and large wave amplitude.

The convergence of the mean heat flux may be calculated from

$$\nabla \cdot \overline{F_T} = \frac{\partial \overline{F_{T_x}}}{\partial x} + \frac{\partial \overline{F_{T_y}}}{\partial y} + \frac{\partial \overline{F_{T_p}}}{\partial p} - \frac{\overline{F_{T_y}}}{a}\tan\varphi \ ,$$

giving

$$\nabla \cdot \overline{F_T} = \delta\frac{C_p km}{2fR}\left(\frac{\sigma_z p(k_T^2 - k^2)}{f\sigma_y(k^2 + k_T^2)}\left(\beta + \frac{f^2}{a^2\beta}\right) - 1\right)\Phi^2 + \frac{C_p}{R}\sigma_y \bar{v}p \ . \tag{2}$$

It will be found in next section that heat balance in geostrophic wave circulations is associated with the convergence of heat flux.

III. HEAT BALANCE IN STATIONARY GEOSTROPHIC WAVES

The primitive equation of thermodynamic energy minus heat perturbation equation (Re-

ferring to Part I) gives the remainder equation of heat:

$$0 = -u'\frac{\partial\alpha'}{\partial x} - v\frac{\partial\alpha'}{\partial y} - \omega'\left(\frac{\partial\alpha'}{\partial p} + \frac{C_v\alpha'}{C_p p}\right) - \sigma_y\bar{v} + \frac{R}{C_p p}H \ . \tag{3}$$

Substituting the stationary geostrophic perturbations into it produces

$$\overline{DT} - \frac{p}{R}\sigma_y\bar{v} + \frac{H}{C_p} + C_1\cos\Psi_s + C_2\sin\Psi_s + D_1\cos 2\Psi_s + D_2\sin 2\Psi_s = 0 \ , \tag{4}$$

where

$$\overline{DT} = \frac{\delta km}{2fR}\left(\frac{\sigma_z p(k^2 - k_T^2)}{f\sigma_y(k^2 + k_T^2)}(\beta + \frac{f^2}{a^2\beta}) + \frac{C_v}{C_p}\right)\Phi^2$$

represents zonal symmetric heating, and

$$C_1 = \frac{\delta\sigma_z k^2 m\bar{v}p}{fR\sigma_y(k^2 + k_T^2)}(\beta + \frac{f^2}{a^2\beta})\ \Phi \ , \tag{5}$$

$$C_2 = -\frac{\delta\sigma_z}{R\sigma_y}m^2\bar{v}p\Phi \ , \tag{6}$$

$$D_1 = \frac{\delta km}{2fR}\left(\frac{\sigma_z p}{f\sigma_y}(\beta + \frac{f^2}{a^2\beta}) + \frac{C_v}{C_p}\right)\Phi^2 \ , \tag{7}$$

$$D_2 = \frac{k}{2fR}\left(\delta^3\frac{\sigma_z}{\sigma_y}m^2 p - \frac{C_v k_T^2}{C_p f(k^2 + k_T^2)}(\beta + \frac{f^2}{a^2\beta})\right)\Phi^2 \ , \tag{8}$$

Taking the zonal average defined in Part I, we rewrite (4) as

$$\overline{DT} - \frac{p}{R}\sigma_y\bar{v} + \frac{\overline{H}}{C_p} + C_1\cos\Psi_s + C_2\sin\Psi_s +$$
$$D_1\cos 2\Psi_s + D_2\sin 2\Psi_s + \frac{H'}{C_p} = 0 \ . \tag{9}$$

The balance relationship of zonal mean heating separated from it gives

$$\overline{DT} - \frac{p}{R}\sigma_y\bar{v} + \frac{\overline{H}}{C_p} = 0$$

and follows, from (2), that

$$\nabla\cdot\overline{F_T} + \overline{\alpha'\omega'} - H = 0 \ .$$

Thus in thermal balance, convergence of heat flux must be cancelled out by diabatic and adiabatic heatings in the atmosphere.

IV. LINEAR AND NONLINEAR RESPONSES

The balance relationship of heat perturbations separated from (9) reads

$$C\cos(\Psi_s - \rho_1) + D\cos(2\Psi_s - \rho_2) = -\frac{H'}{C_p} \ , \tag{10}$$

where

$$C=\sqrt{C_1^2+C_2^2}\ ,$$

$$\cos\rho_1=\frac{C_1}{C}\ ,\qquad \sin\rho_1=\frac{C_2}{C}\ , \tag{11}$$

$$D=\sqrt{D_1^2+D_2^2}\ ,$$

$$\cos\rho_2=\frac{D_1}{D}\ ,\qquad \sin\rho_2=\frac{D_2}{D}\ . \tag{12}$$

Equation (10) tells clearly that the zonal asymmetry of thermal forcing is balanced by the asymmetric generation of heat produced in stationary waves.

To learn the basic mechanism of generating and maintaining thermal stationary waves, we will only consider the idealized forcing represented by a single harmonic function

$$\frac{H'}{C_p}=Q\cos(\tau x+\eta_h)\qquad(\tau>0)\ .$$

For this forcing, the heat generation required by heat balance may also be divided into linear and nonlinear responses, of which phases are determined by

$$\cos(\Psi_s-\rho_1)=-\cos(\tau k+\eta_h)$$

and

$$\cos(2\Psi_s-\rho_2)=-\cos(\tau k+\eta_h)$$

respectively. Thus, the phase of linear response shows

$$\Psi_s=\pm(\tau x-\eta_h)+\rho_1+\pi\ . \tag{13}$$

The zonal wavelength of linear response is the same as that of thermal forcing. While, nonlinear response is in the phase

$$\Psi_s=\frac{1}{2}[\pm(\tau x+\eta_h)+\rho_2+\pi]\ , \tag{14}$$

and has twice the wave length as that of thermal forcing. As shown by (5)–(8), both the linear and nonlinear responses depend strongly on temperature structure of the atmosphere, and their intensities reduce with increasing height when the mean fields and wave parameters are constant. Since decrease of the linear response is more plausible, the nonlinear response may have more contribution at higher levels.

V. THERMAL STATIONARY WAVES AT MIDDLE LATITUDES

An important result obtained from numerical experiments is that horizontal scale of thermal response in the upper troposphere is larger than that of topography below (Held, 1983). From (5) and (6), we find that the linear response is connected with mean meridional flow, and is generally much smaller than the nonlinear response at middle and high latitudes.When thermal stationary waves are induced mainly by nonlinear response, their horizontal scale is twice the scale of thermal forcing.

Without considering linear response, (10) may be replaced by

$$D\cos(2\Psi_s-\rho_2)\approx-\frac{H'}{C_p}\ .$$

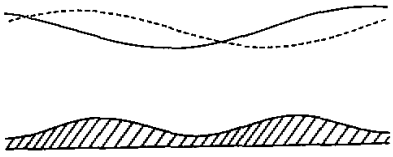

Fig. 1. The stationary geopotential perturbations in the upper troposphere of middle latitudes associated with nonlinear responses to zonally asymmetric thermal forcing during winter (solid line) and summer (dashed line). $\rho_2 = 1.75\ \pi$.

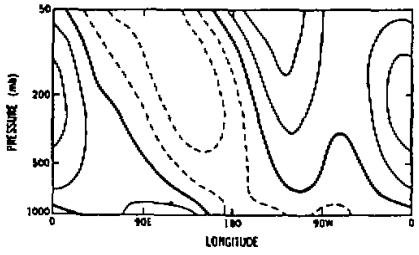

Fig. 2. Longitude–height cross section of perturbation geopotential height at 45°N for linear and nonlinear responses to thermal forcing (After Held, 1983).

From (7) and (8), the square amplitude of induced perturbation is proportional to the intensity of asymmetric thermal forcing. With (14) then, the stationary geopotential field corresponding to the nonlinear response is represented by

$$\varphi'_1 = \begin{cases} -\Phi\sin\frac{1}{2}(\tau x + \eta_h) - \rho_2 & (k > 0) \\ \Phi\sin\frac{1}{2}(\tau x + \eta_h) + \rho_2 & (k < 0) \end{cases}$$

At middle latitudes of the Northern Hemisphere where mean temperature decreases poleward and mean heat flux is downgradient (Newell et al., 1970), we may assume that $k > 0$ and $m > 0$. (The same results may be obtained with the assumption of $k < 0$ and $m < 0$). Therefore, D_1 is usually positive at high levels and D_2 is always negative, so that (12) shows $3\pi/2 < \rho_2 < 2\pi$. Moreover, the positive deviation of temperature from zonal mean takes place over oceans in winter, but over continents in summer. Thus in heat balance, the geopotential perturbations associated with nonlinear response in winter and summer are displayed respectively in Fig.1, together with the idealized topography below.

The thermal contribution may be investigated separately in numerical models. One example is cited in Fig.2, which gives a longitude–height cross section of perturbation geopotential height corresponding to the realistic thermal forcing at 45°N, simulated by Held (1983). In this diagram, linear and nonlinear thermal responses were both involved. The linear response in geopotential field with wave number identical to that of thermal forcing is evident only in the lower troposphere as discussed previously. Whereas, the nonlinear response in the upper troposphere is identified strikingly with wave 1. The similar consequence was also demonstrated by many other authors (e. g., Manabe and Terpstra, 1974; Trenberth, 1983; Jacqmin and Lindzen, 1985 and Tokioka and Noda, 1986).

In the real atmosphere, effect of thermal forcing may be inspected by comparing the observed stationary waves in different seasons, since the thermal forcing varies greatly with time. The seasonal variations in nonlinear response shown in Fig.1 imply an eastward displacement from winter through summer. However, as seasonal variations in intensity of thermal forcing are also announced, the relative deviation, other than the absolute deviation in geopotential field, will be considered in the following discussions.

Provided that there are N centres in a deviation field of which the centre values are D_i $(i=1,2,\cdots,N)$, the mean deviation of the N systems is calculated by

$$D_m=\sqrt{\frac{\sum_{i=1}^{N}D_i^2}{N}}\ .$$

The relative deviation is defined subsequently as:

$$D_{ri}=\frac{D_i}{D_m}\ .$$

In the Fig.6 of Part I, this eastward displacement of major pressure systems at middle latitudes is obvious. While, variations in relative intensities of these systems may be predicted from Fig.1 as well. Regarding the high topography in the left part of the diagram as the Tibetan Plateau again, we may expect that in summer the ridge in the upstream of the Tibetan Plateau will be intensified greatly, and the trough in the downstream weakened; the reverse changes take place respectively in the high and low systems near Rocky Mountains. Moreover, the ridge over the east coast of North Africa will be weakened. This anticipation is verified dramatically by the table below.

Table 1. Seasonal Variations in Planetary Stationary Waves

Systems	H_T	L_T	H_R	L_R	H_A
Intensity (winter)	+60	−260	+180	−120	+180
Intensity (summer)	+300	−300	+60	−180	+20
D_r (winter)	0.346	−1.449	1.038	−0.692	1.038
D_r (summer)	1.442	−1.442	0.288	−0.865	0.096
Displacement	+10	+60	+40	+15	−10
Rv	3.168	−0.005	−0.723	0.250	−0.907

Here, H stands for high and L for low; subscripts T, R, and A relate the H and L to the Tibetan Plateau, Rocky Mountains and the east coast of North Africa, respectively; "+" followed by a magnitude of longitude on the line of displacement directs eastward, and "−", westward. Rv measures the relative variations in the relative intensities defined as:

$$R_v=\frac{D_r(\text{summer})-D_r(\text{winter})}{D_r(\text{winter})}\ .$$

A positive Rv means intensification, while a negative value indicates relative abatement. This table shows that the expected large intensification really occurs in H_T and H_R. While, as L_T moves farthest to the east, the smallest change in its relative intensity is made. Moreover, for H_A displaces westward, its abstement is greater than expected.

VI. SUBTROPICAL STATIONARY WAVES

The observed subtropical highs are usually not zonally symmetric in both hemispheres. So, asymmetry of topography may also have great contribution on the stationary waves in the subtropical regions. We will find, in particular, that influence of thermal forcing may be more remarkable than that at middle and high latitudes, especially in summer time, since orographic slopes in the subtropics are generally smaller.

1. *In the Summer Season*

Fig.3 gives the longitude–hight cross sections of the stationary geopotential height observed at 25°N and 25°S in summer. The first common characteristic of the subtropical stationary waves in both hemispheres is that they have the scale similar to that of asymmetric topography in the same hemisphere. The second one is that the wave phases in the upper troposphere are just opposite to those in the lower troposphere, while the maximum amplitudes are almost the same. These characteristics intimate that the stationary waves are mainly associated with linear response to thermal forcing, because the mean meridional flows are towards opposite directions in the upper and lower branches of Hadley cells.

As the mean meridional circulation in Hadley cells is usually stronger than in Ferrel cells at low latitudes' and amplitude of the geopotential perturbatioon there is less than at higher latitudes' the linear response may be more significant than nonlinear response for the subtropical stationary waves. The linearly induced stationary geopotential perturbation is represented by

$$\varphi'_1 = \begin{cases} -\Phi\sin(\tau x + \eta_h) - \rho_1 & (k > 0) \\ \Phi\sin(\tau x + \eta_h) + \rho_1 & (k < 0) \end{cases}$$

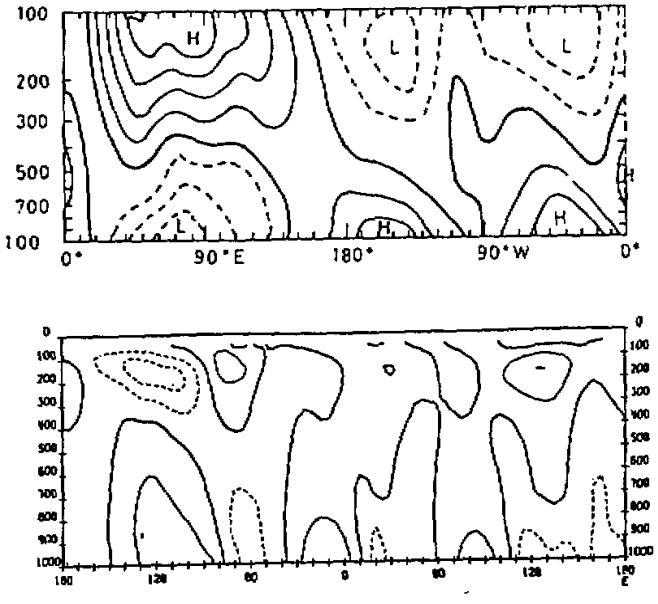

Fig.3. Longitude–height cross sections of stationary wave geopotential height for the summer season at (a) 25°N and (b) 25°S, respectively. Contour interval 30 m. The zero contour is thickened (After Wallace, 1983).

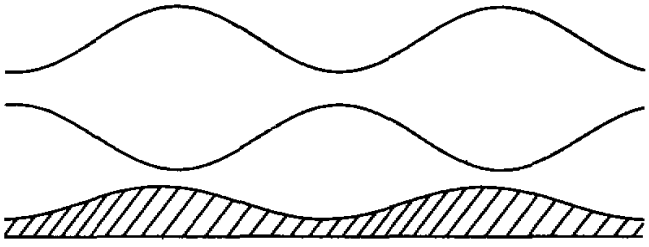

Fig.4. The stationary geopotential perturbations associated with linear response of thermal forcing in the subtropical regions during summer. Perturbations in the upper and lower branches of Hadley cells are represented by the upper line ($\rho_1 = 0.6\pi$) and lower line ($\rho_1 = 1.6\pi$), respectively.

When the wave flux of heat is downgradient in the Northern Hemisphere subtropics, we may assume that $k > 0$ and $m > 0$ (or equivalently $k < 0$ and $m < 0$). Consequently, we have $\pi/2 < \rho_1 < \pi$ in the upper branch of Hadley cells and $3\pi/2 < \rho_1 < 2\pi$ in the lower branch. Referring to Part I, we see that K_T^2 may be very large in the almost barotropic regions, so $\mathrm{ctg}\rho_1$ is close to zero. If ρ_1 is assigned to be 0.6π and 1.6π at upper and lower levels, respectively, the stationary geopotential perturbations forced linearly by thermal forcing over the idealized topography in the summer subtropics may be sketched in Fig. 4, when heat balance is established.

In the subtropics of the Southern Hemisphere we assume, for the downgradient wave flux of heat, that $k > 0$ and $m < 0$ (or $k < 0$ and $m > 0$). So the stationary geopotential waves corresponding to the linear thermal response are illustrated also by Fig.4. The similarity of this diagram to observations may be examined by comparing with Fig.3.

As stationary waves in the subtropical regions depend greatly on thermal forcing and mean thermal structure, seasonal changes in these waves must be greater than those at middle and high latitudes. Thus, subtropical stationary waves in the winter season may be largely different as discussed below.

2. *In the Winter Season*

During winter time, zonal asymmetry of thermal forcing is much weaker than in summer in the subtropical regions. This may be seen clearly by comparing the Longitude–height cross sections of temperature at 25° of both hemispheres (Wallace, 1983). Therefore, the linear response to thermal forcing in the winter subtropics is reduced, so that linear orographic effect may become more notable, especially at high levels of the Northern Hemisphere.

As mean westerlies around mountain height are generally weak but ageostrophic motions are relatively large in the subtropical regions, equations (24), (25) and (29) in Part I show $\sin\varphi_1 > 0$ with $k > 0$ and $m > 0$. The phase of stationary geopotential perturbations may be displayed in Fig.5 for both $\cos\gamma_1 > 0$ and $\cos\gamma_1 < 0$, respectively. These distributions can be confirmed by referring to Fig.6 in Part I. The linear orographic effect near 20°N is remarked by the closed lows on the windward sides of Rocky Mountains and the Tibetan Plateau, which are preceded by ridges on the lee sides of these mountain ranges.

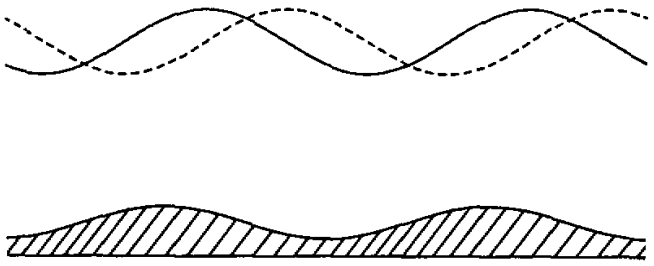

Fig.5. The stationary geopotential perturbation corresponding to linear orographic response in the subtropical regions. The solid line is for $\gamma_1 = 0.25\pi$, while the dashed line is for $\gamma_1 = 0.75\pi$.

In the Southern Hemisphere, both the thermal and orographic forcings are weak during winter, so the stationary perturbations in the subtropics of the Southern Hemisphere winter may be associated, to the same extent, with both thermal and orographic effects. Also, either the linear or nonlinear response may be of similar significance on the stationary waves. So it is generally difficult to distinguish clearly one particular response from the others in long-term averaged perturbation fields.

VII. THERMAL STATIONARY WAVES IN THE LOWER TROPOSPHERE

The stationary waves below 700 hPa at middle and higher latitudes in the Northern Hemisphere show a pronounced westward tilt with height in the winter (Wallace, 1983; see also the Fig.4 in Part I). While, the observed summertime stationary waves have the prevailing tendency for an eastward slope with height in the lower troposphere. The westward tilt is generally more plausible than the eastward tilt. These seasonal variations imply that the stationary waves in the lower troposphere are excited by thermal forcing. Since asymmetric thermal forcing near the surface is larger than above, it will be considered in perturbation equations. When vertical motion is ignored, the non-divergence and steady perturbation equations without using small-oscillation approximation are given by

$$\bar{u}\frac{\partial u'}{\partial x} - fv' = -\frac{\partial \varphi'_1}{\partial x} \ , \tag{15}$$

$$\bar{u}\frac{\partial v'}{\partial x} + fu' = -\frac{\partial \varphi'_1}{\partial y} \ , \tag{16}$$

$$\frac{\partial \varphi'_1}{\partial p} = -\alpha' \ , \tag{17}$$

$$\bar{u}\frac{\partial \alpha'}{\partial x} + \sigma_y v' = \frac{RH'}{C_p p} \ . \tag{18}$$

If we introduce a streamfunction ψ:

$$u' = -\frac{\partial \psi}{\partial y} \ , \qquad v' = \frac{\partial \psi}{\partial x} \ ,$$

(15) and (16) may be replaced by the vorticity equation

$$\bar{u}\frac{\partial}{\partial x}\nabla^2\psi + \beta\frac{\partial \psi}{\partial x} = 0 \ .$$

Provided that

$$\psi = \mathrm{r}(p)\sin(kx - my) \ ,$$

where $\mathrm{r} > 0$, it gives

$$k^2 + m^2 = \frac{\beta}{\bar{u}} \ .$$

Moreover, since

$$u' = \mathrm{r}(p)m\cos(kx - my) \ ,$$
$$v' = \mathrm{r}(p)k\cos(kx - my) \ .$$

we gain the perturbation geopotential field, from (15) and (16),

$$\varphi'_1 = f\mathrm{r}(p)\sin(kx - my) - \bar{u}m\mathrm{r}(p)\cos(kx - my) \ .$$

Consequently, (17) and (18) produce

$$H' = \frac{C_p}{R}kp[(\sigma_y \mathrm{r} - f\bar{u}\mathrm{r}_p)\cos(kx - my) - \bar{u}^2 m\mathrm{r}_p \sin(kx - my)] \ .$$

It follows that

$$\frac{C_p}{R}Ap\cos(kx - my - \mu_1) = H' \ ,$$

in which, $\mathrm{r}_p = \partial \mathrm{r} / \partial p$ and

$$A = \sqrt{(\sigma_y \mathrm{r} - f\bar{u}\mathrm{r}_p)^2 + \bar{u}^4 m^2 \mathrm{r}_p^2} \ ,$$

$$\cos\mu_1 = \frac{\sigma_y \mathrm{r} - f\bar{u}\mathrm{r}_p}{A} \ , \qquad \sin\mu_1 = -\frac{\bar{u}^2}{A}m\mathrm{r}_p \ . \tag{19}$$

If the zonally asymmetric thermal forcing is idealized again by

$$H' = Q(p)\cos(\tau x + \eta_h) \ ,$$

we may see

$$\frac{C_p Akp}{R}\cos(kx - my - \mu_1) = Q(p)\cos(\tau x + \eta_h) \ .$$

It produces

$$\sqrt{(\sigma_y \mathrm{r} - f\bar{u}\mathrm{r}_p)^2 + \bar{u}^4 m^2 \mathrm{r}_p^2} - \frac{RQ(p)}{C_p kp} = 0 \ , \tag{20}$$

and

$$kx - my = \pm(\tau x + \eta_h) + \mu_1 \ .$$

Therefore,

$$\varphi'_1 = \begin{cases} G\mathrm{r}\sin(\tau x + \eta_h + \mu_1 + \mu_2) & (k > 0) \\ -G\mathrm{r}\sin(\tau x + \eta_h - \mu_1 - \mu_2) & (k < 0) \end{cases} \tag{21}$$

where

$$G = \sqrt{f^2 + \bar{u}^2 m^2} \ ,$$

$$\cos\mu_2 = \frac{f}{G} \ , \qquad \sin\mu_2 = -\frac{\bar{u}m}{G} \ . \tag{22}$$

Now, the perturbation geopotential field forced thermally in the lower troposphere is expressed approximately by (21). The amplitude is determined by (20), while the phase depends on thermal forcing, mean circulation structure and wave parameters.

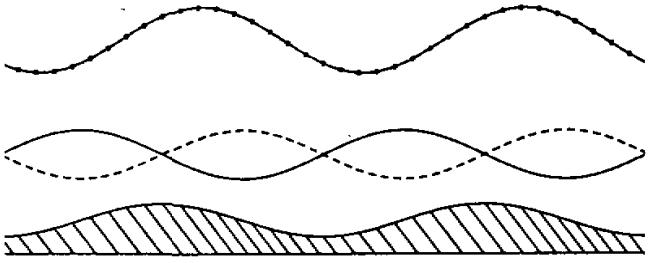

Fig.6. The geopotential perturbations of thermal Rossby waves at middle latitude of the Northern Hemisphere ($\mu_1 + \mu_2 = 3\pi$). Solid line is drawn for winter, and dashed line for summer. The upper geopotential perturbation is depicted by dotted line.

For these low–level thermal Rossby waves, we may suppose $r_p > 0$. Since heat flux is poleward at middle latitudes of the Northern Hemisphere, we adopt positive k and m (or negative equivalently) for relationships (19) and (22), showing $\pi < \mu_1 < 3\pi/2$ and $3\pi/2 < \mu_2 < 2\pi$ respectively in mean westerlies. Thus, $2.5\pi < \mu_1 + \mu_2 < 3.5\pi$.

Furthermore,

$$\mu_1 + \mu_2 = \arctan\left(-\frac{\bar{u}^2 m r_p}{\sigma_y r - f\bar{u} r_p}\right) + \arctan\left(-\frac{\bar{u}m}{f}\right)$$

$$= \arctan\left(-\frac{\bar{u}\sigma_y m r}{f(\sigma_y r - f\bar{u} r_p) - \bar{u}^3 m^2 r_p}\right).$$

Thus, for large scale perturbations, $\tan(\mu_1 + \mu_2)$ is close to zero, and so $\mu_1 + \mu_2 \approx 3\pi$. When $\mu_1 + \mu_2 = 3\pi$ is used, the geopotential perturbations in the lower troposphere at middle latitudes during winter and summer are demonstrated respectively in Fig.6. For comparison, the orographically forced stationary geopotential perturbation at high levels is depicted by dotted line, which is the same as the solid line in Fig.3 of Part I. This figure shows clearly that the phases of stationary thermal Rossby wave displace eastward in winter, but westward in summer. So the observed stationary waves in the lower troposphere manifest the westward and eastward tilts with height, respectively, during winter and summe. Fig.6 shows that the westward tilt in winter is more notable than the eastward tilt in summer.

VIII. CONCLUSIVE REMARKS

It is made clear that existence of thermal stationary waves is necessary for long–term heat balance in the atmosphere with asymmetric thermal forcing below. The thermal waves at middle latitudes, especially in high levels, are associated mostly with nonlinear response. This response having twice the scale as relevant forcing and so being more responsible for existence of wave 1, makes considerable modifications on the orographic stationary waves and may explain the seasonal changes in observed stationary waves. Unlike the orographic effect discussed in Part I, thermal contribution is essentially baroclinic, and hence can only be simulated realistically by baroclinic and nonlinear models.

In the summer subtropical regions of both hemispheres, where Hadley cells are strong and mean westerlies are weakened, linear thermal response may have a great effect on sta-

tionary waves. So the stationary waves there show the opposite phase distributions at high and low levels respectively. Also, stationary waves in these regions are more sensitive to variations of thermal forcing and exhibit more remarkable seasonal changes.

In the lower troposphere particularly below 700 hPa, thermal forcing is strong at middle latitudes of the Northern Hemisphere, so that it may produce stationary thermal Rossby waves. The phases of these waves displace to the east and west in winter and summer respectively, compared with the orographically forced stationary waves at higher levels.

Similarly to the orographic waves, distributions of thermal stationary waves depend on mean circulation fields, heat and momentum fluxes as well as external forcing. So the stationary waves cannot be simulated realistically by the models restricted in a limited channel. In general, direction of heat or momentum flux and the mean circulation structure change with latitude in both hemispheres, so phases of stationary waves may be meridionally asymmetric over the same topography. This meridional asymmetries do not suggest the meridional propagation of planetary perturbations. When stationary waves at middle latitudes and subtropics are separated by a subtropical westerly jet near the tropopause, the cores of this jet take place spontaneously between troughs and ridges with ridges equatorward. For example at 200 hPa of the Northern Hemisphere, they are over the east side of continents and to the south of the major troughs at middle latitudes (James, 1983).

I wish to thank C. N. Duncan, K. J. Weston, and R. S. Harwood for their helpful comments and encouragements.

REFERENCES

Held, I. M. (1983), Stationary and quasi-stationary eddies in the extratropical troposphere: theory, In *Large-Scale Dynamical Processes in the Atmosphere* (B. J. Hoskins and R. P. Pearce, Eds), Academic Press, 127–168.

Jacqmin, D. and R. S. Lindzen (1985), The causation and sensitivity of the Northern winter planetary waves, *J. Atmos. Sci.*, **42**: 724–745.

James, I. N. (1983), Some aspects of the global circulation of the atmosphere in January and July 1980, In *Large-Scale Dynamical Processes in the Atmosphere* (B. J. Hoskins and R. P. Pearce, Eds), Academic Press, 5–25.

Manabe, S. and T. B. Terpstra (1974), The effects of mountains on the general circulation of the atmosphere as identified by numerical experiments, *J. Atmos. Sci.*, **31**: 3–42.

Newell, R. E., et al. (1970), The energy balance of the global atmosphere, In *The Global Circulation of the Atmosphere*, G. A. Corby, ed., London, Royal Meteorological Society, 42–90.

Smagorinsky, J. (1953), The dynamical influence of large-scale heat sources and sinks on the quasi-stationary mean motions of the atmosphere, *Quart. J. Roy. Met. Soc.*, **79**: 342–366.

Tokioka, T. and A. Noda (1986), Effects of large scale orography on January atmospheric circulation: A numerical experiment, *J. Meteor. Soc. Japan.* **64**: 819–839.

Trenberth, K. E. (1982), Seasonality in Southern Hemisphere eddy statistics at 500 hPa, *J. Atmos. Sci.*, **39**: 2507–2520.

Trenberth, K. E. (1983), Interactions between Orographically and thermally forced planetary waves, *J. Atmos. Sci.*, **40**: 1126–1153.

Wallace, J. M. (1983), The climatological mean stationary waves: observational evidence, In *Large-Scale Dynamical Processes in the Atmosphere* (B. J. Hoskins and R. P. Pearce, Eds), Academic Press, 27–54.